DOI: 10.61782/fa.2023.1054

forum acusticum 2023

# ASSESSMENT OF THE DIRECTIONAL CHARACTERISTICS OF THE EAR CANAL USING 3D PRINTED REPLICAS AND NUMERICAL SIMULATIONS

**Daniel Sinev**[1,2*] **Fabio Di Giusto**[3,4] **Katharina Pollack**[5]
**Kurt Mick**[1] **Jürgen Peissig**[2]
[1] Sonova Consumer Hearing GmbH, Wedemark, Germany
[2] Institut für Kommunikationstechnik, Leibniz Universität Hannover, Germany
[3] KU Leuven, Department of Mechanical Engineering, Heverlee, Belgium
[4] Flanders Make@KU Leuven
[5] Acoustics Research Institute, Austrian Academy of Sciences, Vienna, Austria

## ABSTRACT

In modern literature it is generally assumed that ear canals have little to no effect on the directional components of head-related transfer functions and thus, on spatial perception of sound. Therefore, in most spatial audio applications today, sound propagation is only considered up to the blocked entrance of the ear canal. To challenge this assumption, a study was conducted using custom-made 3D printed replicas of a subject's outer ears including complete ear canals with microphones embedded at the eardrum position. The replicas were mounted in a cheek simulator and set up on a rotary table in an anechoic chamber. Transfer functions from an external source to both the ear canal entrance and to the eardrum positions were measured. Measurement data were acquired for the horizontal and the frontal planes. Using these to validate simulation parameters, transfer functions from other directions were calculated through numerical simulations. The effect of the direction of arrival on ear canal transmission was estimated. Study findings are compared to and contrasted against previous studies carried out on real human ears.

**Keywords:** *ear canal, spatial audio, HRTFs*

*__Corresponding author__: *daniel.sinev@gmail.com.*


## 1. INTRODUCTION

In spatial audio rendering over headphones, accurate Head-Related Transfer Functions (HRTFs) are necessary for correct perception of sound localisation and immersion [1,2]. Nowadays HRTFs are usually measured and/or simulated up to a microphone placed at the entrance of a blocked ear canal, which assumes that ear canal transmission is directionally independent [2, 3]. While several studies exist that support this assumption [4–8], we would like to challenge it in this paper with the help of a new approach.

Studies involving acoustic measurements in human ears are challenging due to the human factor. It is not easy to fix the precise measurement positions, which leads to repeatability issues. This can cause high measurement uncertainty, as well as limit the amount of data that can be reliably acquired. For instance, while in [6] the authors measured source positions covering the full sphere at 10 degree resolution, their data does not include measurements at the eardrum. Conversely, in [7], several positions inside the ear canal were investigated, including at the eardrum, but only three directions of arrival were captured.

In this study, thanks to a recently published database of human geometries including ear canals up to the eardrum [9], we were able to manufacture precise replicas of a pair of human outer ears, including pinnae and complete ear canals. This allowed us to perform highly

repeatable measurements as well as to have the same geometry available for simulations. Furthermore, microphones were embedded into the replicas at the eardrum positions. This way, accurate data could be acquired at as many source positions as desired. Although these replicas do not exactly reflect the acoustic behaviour of real ears due to mismatches in material properties and the lack of a movable eardrum, they allow for precise comparison of HRTFs measured on real human geometries with microphones located at the ear canal entrance to those measured at the eardrum position, and thus investigate the directional dependence of ear canal transmission. This paper constitutes one part of a three-paper study based on these replicas and their geometries (see [10, 11]).

## 2. METHODS

### 2.1 Manufacturing ear replicas

Full outer ear replicas with ear canals were produced using the randomly chosen 9$^{th}$ subject from the IHA database of human geometries [9]. The replicas were manufactured in two parts, with 3D printed pinnae and silicone inner ear canals (Fig. 1a). The pinnae parts were printed in two materials, one rigid and one flexible, to study the effect of their acoustic impedance. Only rigid pinnae measurements are presented in this paper, while the effect of the material choice is investigated in [10].


(a) Full replica mounted on a cheek simulator

(b) Inner ear canal with an integrated microphone

**Figure 1**: 3D printed ear replica

Using modified negatives of the ear canals and silicone casting, calibrated Sennheiser KE-4 microphone capsules were embedded at the eardrum positions (Fig. 1b). The full description of the manufacturing process can be found in [12].

### 2.2 Measurements

Measurements were performed in an anechoic chamber with a cut-off frequency of 100 Hz, using a computer-controlled turntable and a full audio bandwidth measurement loudspeaker embedded into the chamber wall. With the ear replicas mounted onto a GRAS 43AG cheek simulator positioned in the far field, 1.66m away from the source, horizontal (Fig. 2a) and frontal plane (Fig. 2b) measurements were performed with a 5 degree resolution. The frontal plane rather then the more usual median plane was chosen due to it having more variation in incidence angles with respect to the ear canal. Only the ipsilateral half-spheres were covered, since contralateral measurements would not be representative for an ear replica without an artificial head. Two sets of measurements were acquired for each ear, one using the integrated eardrum microphones, and another using DPA 4560 CORE Binaural Headset Microphones at the ear canal entrance positions. The measurements were repeated, first without changing the setup, and then repositioning the binaural microphones by taking them out and putting them back in.

All measurements were performed using sine sweeps in the bandwidth from 100 Hz to 20 kHz. Reference measurements using the binaural microphones and matching calibrated KE-4 capsules, but without the ear replicas present (Fig. 2c), were recorded to perform free-field equalisation as defined in [1] by dividing the measured complex spectra $S_i$ by the reference spectrum $S_{ref}$. These free-field equalised transfer functions are further referred to as Pinna-Related Transfer Functions, or PRTFs, $PRTF_i = S_i/S_{ref}$.

(a) Horiz. plane

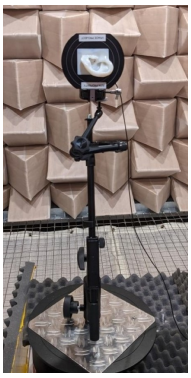

(b) Frontal plane

(c) Ref. meas.

**Figure 2**: Anechoic chamber: measurement setup

### 2.3 Simulations

Taking the same geometries that were used to manufacture the replicas, matching PRTFs were also acquired via free-field FEM simulations in COMSOL®. In addition to the measurement positions, the ipsilateral half-spheres were covered at 5 degree resolution in both azimuth and elevation. Three microphone positions were considered: at the eardrum, at the binaural microphone positions keeping the ear canal open, and blocking the ear canals at the position matching the binaural microphones. The simulations were performed with rigid boundary conditions (BCs) as well as using measured acoustic impedances of the materials, of which a more detailed description can be found in [10]. The simulations using impedance boundary conditions produce results that are significantly closer to the measurements around resonances (example shown in Fig. 3), so only they are used in this study. Here and below all graphs are plotted in 1/96th octave resolution.

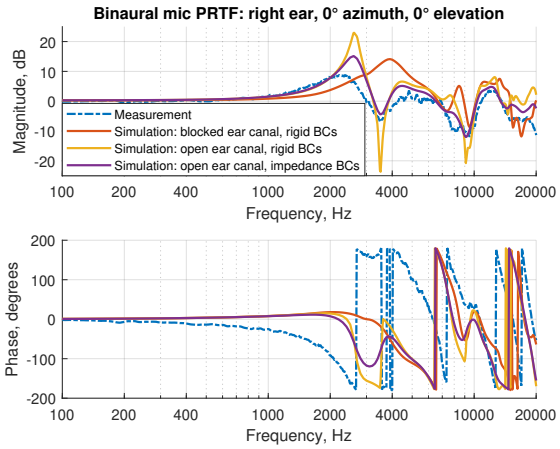


**Figure 3**: Simulated vs measured PRTF: binaural mic position, example for one direction

Another important note is that, while it was originally supposed that the binaural microphones would block the ear canal, it is clear when comparing measurements to simulations (Fig. 3) that their response is much closer to the open ear canal case. Indeed, after subsequent examination it became apparent that not only is the foam fitted onto the binaural microphones quite acoustically transparent, but it also does not fully block the ear canal when inserted. To investigate the effect of keeping the ear canal open, both sets of simulations, with blocked and open ear canals, were kept for processing.

### 2.4 Choice of metric

In order to study the dependence of ear canal transmission on the direction of arrival, an objective metric is necessary. Firstly, the ear canal transmission is estimated by the difference between eardrum PRTFs ($PRTF_{ed}$) and binaural PRTFs ($PRTF_{bin}$), as calculated in eq. 1, producing a $PRTF_{dif}$ for each direction. Since both PRTF measurements are performed using the same setup except for the position of the microphone, calculating their ratio cancels out the response of the cheek simulator, isolating the ear canal effects. To further simplify the results, diffuse-field equalisation can be used [2], resulting in Directional Transfer Functions, or DTFs (eq. 2). Index $i$ here stands for the incidence angles, with $N_i$ as the number of directions of arrival in a given dataset. Since Common Transfer Functions, or CTFs, (eq. 2), are directionally independent, ear canal transmission differences $DTF_{dif}$, calculated with DTFs instead of PRTFs, will still have the same dependence on direction (eq. 3).

$$PRTF_{dif,\,i} = \frac{PRTF_{ed,\,i}}{PRTF_{bin,\,i}} \tag{1}$$

$$DTF_i = \frac{PRTF_i}{CTF}, \quad CTF = \frac{\sum_i (PRTF_i)}{N_i} \tag{2}$$

$$DTF_{dif,\,i} = \frac{DTF_{ed,\,i}}{DTF_{bin,\,i}} = PRTF_{dif,\,i} \cdot \frac{CTF_{bin}}{CTF_{ed}} \tag{3}$$

The CTFs calculated from right ear measurements are shown in Fig. 4, computed with minimum phase to avoid non-causal DTFs. Although the direction sampling here is not spherically uniform, and these CTFs are thus not strictly correct, ear canal resonances can be clearly seen in them, with a positive quarter-wave resonance at the eardrum and a negative half-wave resonance at the ear canal entrance.

Once the per-direction $DTF_{dif}$ is calculated, a metric needs to be chosen to quantify the effect of the direction of arrival. One option is to calculate the maximum Spectral Difference ($SD_{max}$), which shows the total spread of dB values per frequency (eq. 4). Since this is very sensitive to outliers, a more usual metric is the Directional Spread ($DS$), defined in [7] as the standard deviation ($\sigma$) of the magnitude in dB of the ear canal transmission difference, calculated over the incident angles $i$ (eq. 5). Both are shown in Fig. 5, taking the right ear measurements as an example.

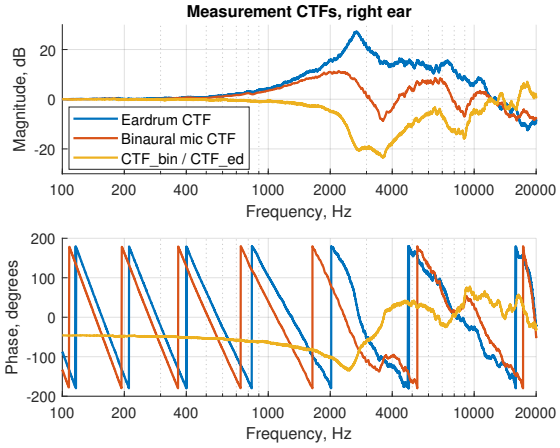


**Figure 4**: Measured right ear CTFs

In order to be consistent with previous research, directional spread is used as the main assessment metric of this study.

$$SD_{max} = \max_{i,j} \left( 20 \cdot \log_{10} \frac{|DTF_{dif,\,i}|}{|DTF_{dif,\,j}|} \right) \quad (4)$$

$$DS = \sigma_i \left( 20 \cdot \log_{10} |DTF_{dif}| \right) \quad (5)$$

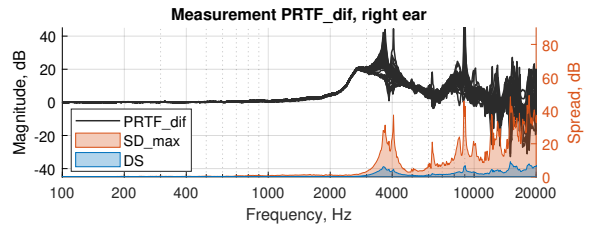


(a) $PRTF_{dif}$ calculation

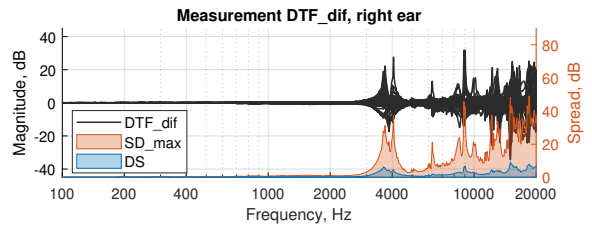


(b) $DTF_{dif}$ calculation

**Figure 5**: Measured right ear: $SD_{max}$ and $DS$

## 3. RESULTS

### 3.1 Measurements

#### *3.1.1 Experimental spread*

In reality, a calculated directional spread will include two components: the true directional dependency, and any errors due to measurement uncertainty. However, repeated measurements with the same source position would create the same errors as when the source position is changed. Thus, in the hypothesis of zero directional dependency of the ear canal, measured directional spread would not be equal to zero, but rather equivalent to the experimental Spread ($ES$), defined in [7] as the standard deviation of the dB magnitude of measurement repetitions ($\sigma_{rep}$) averaged across the directions of arrival (eq. 6). A comparison between the two metrics can be used to verify the existence of a true directional spread. The negative conclusions in [7] are based on them matching, as can be seen in Fig. 6.

$$ES = \frac{\sum_i \left( \sigma_{rep} \left( 20 \cdot \log_{10} |DTF_{dif,i}| \right) \right)}{N_i} \quad (6)$$

Fig. 6 also shows our calculated experimental spread for two cases: a $DTF_{dif}$ measurement that was repeated without modifying the setup, and another where the binaural microphone was taken out and put back in, repositioning it slightly. The significantly lower values from our experiment are consistent with a higher repeatability of our setup compared to measurements on human ears, although more repetitions and ideally more ear geometries would provide higher confidence in these results.

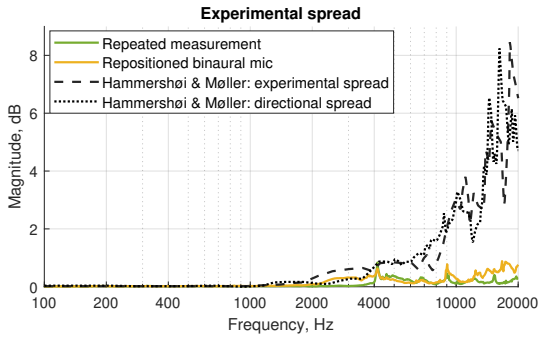


**Figure 6**: Experimental spread: repeated vs repositioned vs Hammershøi and Møller

### 3.1.2 *Directional spread*

Directional spread was calculated separately for the right and the left ears, because they show significantly different behaviour (Fig. 7).

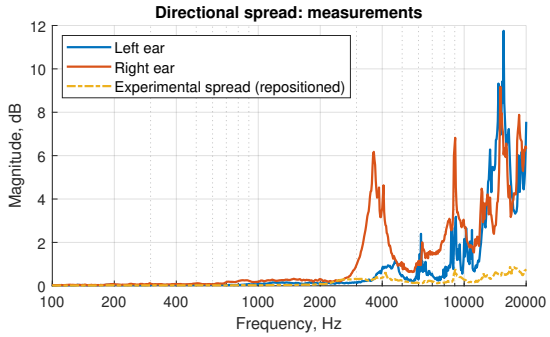


**Figure 7**: Directional spread: measurements

While being similar at high frequencies, particularly above 10 kHz, the right ear directional spread has a 6dB peak around 3.6-4 kHz, which is not present in the left ear measurements. Additional peaks at 9 kHz and 15kHz, which might be harmonically related to the first one, are present in both left and right ear results, albeit at different amplitudes. These results persist for measurements repeated after repositioning the binaural microphones. While the reason for this discrepancy is not readily apparent, a possible explanation is offered in section 4.

## 3.2 Simulations

### 3.2.1 *Measurement dataset*

As described in section 2.3, the simulations were performed for source positions covering the ipsilateral half-spheres for each ear. However, in order to make a direct comparison, a sub-set of source positions on the horizontal and frontal planes, matching the measurement dataset, was analysed first.

Fig. 8 shows the comparison between the measurement and the simulation results for matching source positions. Curiously, both the open and the blocked ear canal simulations follow the left ear measurements much better than the right ear ones. However, the open ear canal simulations do include similar series of peaks in the vicinity of 4 kHz, 9 kHz and 15 kHz. While they don't reach the amplitude of the ones from the measurement data, their frequencies are consistent enough to suggest a link.

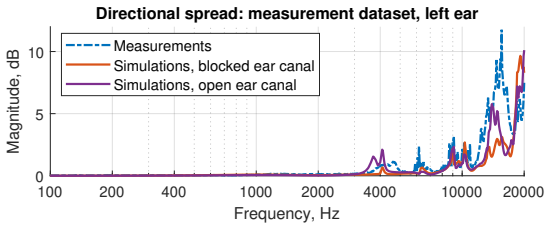


(a) Left ear

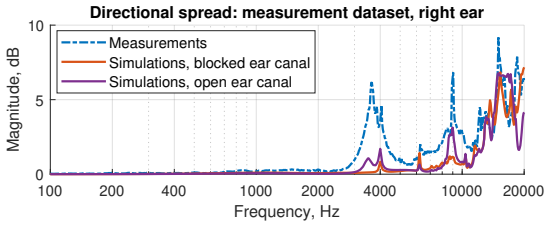


(b) Right ear

**Figure 8**: Directional spread: simulations vs measurements, same source positions

### 3.2.2 *Full dataset*

When calculating the directional spread of the full simulation dataset by combining the two half-spheres from the left and the right ear data, the difference between blocked and open ear canal simulations becomes more apparent. As can be seen in Fig. 9, the directional spread of the open ear canal simulations have a peak series comparable to that of the right ear measurements, while the blocked ear canal simulations do not.

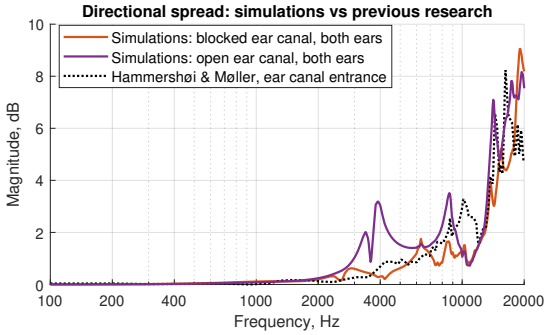


**Figure 9**: Directional spread: simulations vs Hammershøi & Møller

It also shows a comparison of the simulation results

to the data extracted from [7]. They match the blocked ear canal simulations quite well below 9 kHz, but curiously, have additional peaks around 10 kHz, 14 kHz, and 16 kHz.

## 4. DISCUSSION

Two significant features can be isolated in the results of this study. The first, as discussed in the previous section, is the presence of a peak series around 4 kHz, 9 kHz and 15 kHz in the directional spread of (mainly) the right ear measurements and of the open ear canal simulations (Fig. 7-9). The second is the fact that while directional spread results are consistent with previous research (apart from the 4 kHz peak), our experimental spread values are much lower at frequencies above 5 kHz (Fig. 6).

The peak series discrepancy might be explained by the following considerations: firstly, its frequencies match the half-wave resonances of a tube roughly the length of the ear canal, and secondly, it is only present in open ear canal simulations. Since no peak has been observed around 4 kHz in previous research involving human ears, our conclusion is that it must be due to a directionally dependent open ear canal resonance, present in the replicas because of their low acoustic damping compared to real ears. It is possible that this effect is present in real ears as well, but with the higher damping, the resonance would be much smaller and would not result in an observable effect, except at higher frequencies (Fig. 9).

While these assumptions alone do not explain the lack of the 4 kHz peak in left ear measurements, it is probable that the binaural microphone was obscuring the ear canal better in that case, leading to results more closely resembling those typical of a blocked ear canal behaviour. Further study is needed, including measurements with properly blocked ear canals, e. g. using the technique described in [3].

The more interesting finding of this study is the difference between the directional and the experimental spreads, which was not observed in any of the previous studies [4–8]. The observed lower experimental spread is consistent with our assumption that the ear replicas used in our study would provide highly repeatable measurements compared to human subjects. Moreover, a similar trend is present in simulation results (Fig. 9), which, at least in theory, have no experimental spread. This indicates a significant directional dependence of ear canal transmission at frequencies above 5 kHz.

Whether or not this high-frequency directional dependence can make a difference to perception is not yet clear. In [11] we begin to investigate this question by applying a perceptual model to HRTFs simulated on head geometries from [9].

## 5. CONCLUSIONS

Using a pair of full outer ear replicas, directional measurements were conducted in an anechoic chamber, with binaural microphones at the ear canal entrances and microphone capsules embedded at the eardrum positions. Simulations were performed on the same ear geometries, extending the source position dataset to a full sphere with a 5 degree resolution in both azimuth and elevation.

Both sets of acquired data were processed to obtain the directional spread, a metric quantifying the directional dependence of ear canal transmission. This was contrasted against the experimental spread to control for repeatability errors. Two discrepancies were observed: a peak series around 4, 9 and 15 kHz present in some datasets, and a significant difference between the directional and experimental spreads at frequencies above 5 kHz. The first is most likely due to the experiment setup and can likely be eliminated by performing binaural measurements with properly blocked ear canals. The second discrepancy, however, provides a strong indication of existing directional dependence of ear canal transmission at higher frequencies.

Since the low number of repetitions and the fact that only a single pair of ears was used could have affected our results, a further investigation with a more rigorous repeatability analysis and more subject geometries is planned. The ears will also be mounted on an artificial head to include source positions from the contralateral half-spheres.

## 6. ACKNOWLEDGMENTS

This project has received funding from the European Union's Horizon 2020 research and innovation programme under the Marie Skłodowska-Curie grant agreement No 812719.

We would also like to thank the team at the Institut für Kommunikationstechnik, Leibniz Universität Hannover, for providing the facilities and equipment, as well as the team at the chemical lab of Sennheiser electronic GmbH & Co. KG, who were instrumental in the manufacturing of the ear replicas.

## 7. REFERENCES


[1] H. Møller, "Fundamentals of binaural technology," *Applied Acoustics*, vol. 36, no. 3-4, pp. 171–218, 1992.

[2] S. Li and J. Peissig, "Measurement of Head-Related Transfer Functions: A Review," *Applied Sciences*, vol. 10, p. 5014, Jan. 2020.

[3] K. Pollack, W. Kreuzer, P. Majdak, K. Pollack, W. Kreuzer, and P. Majdak, *Perspective Chapter: Modern Acquisition of Personalised Head-Related Transfer Functions – An Overview*. IntechOpen, Apr. 2022. Publication Title: Advances in Fundamental and Applied Research on Spatial Audio.

[4] F. M. Wiener and D. A. Ross, "The Pressure Distribution in the Auditory Canal in a Progressive Sound Field," *The Journal of the Acoustical Society of America*, vol. 18, pp. 401–408, 1946.

[5] E. A. G. Shaw, "Acoustic Response of External Ear with Progressive Wave Source," *The Journal of the Acoustical Society of America*, vol. 51, p. 150, 1972.

[6] J. C. Middlebrooks, J. C. Makous, and D. M. Green, "Directional sensitivity of sound-pressure levels in the human ear canal," *The Journal of the Acoustical Society of America*, vol. 86, pp. 89–108, July 1989.

[7] D. Hammershøi and H. Møller, "Sound transmission to and within the human ear canal," *The Journal of the Acoustical Society of America*, vol. 100, no. 1, pp. 408–427, 1996.

[8] V. R. Algazi, C. Avendano, and D. Thompson, "Dependence of Subject and Measurement Position in Binaural Signal Acquisition," *Journal of the Audio Engineering Society*, vol. 47, pp. 937–947, Nov. 1999.

[9] R. Roden and M. Blau, "The IHA database of human geometries including torso, head and complete outer ears for acoustic research," Sept. 2021.

[10] F. di Giusto, D. Sinev, K. Pollack, S. van Ophem, and E. Deckers, "Analysis of Impedance Effects on Head-Related Transfer Functions of 3D Printed Pinna and Ear Canal Replicas," in *Proc. of Forum Acusticum 2023*, submitted, 2023.

[11] K. Pollack, F. di Giusto, D. Sinev, and P. Majdak, "Spectral and psychoacoustic evaluation of head-related transfer functions calculated at the blocked ear canal and the eardrum," in *Proc. of Forum Acusticum 2023*, submitted, 2023.

[12] D. Sinev, F. di Giusto, J. Peissig, S. van Ophem, and E. Deckers, "Individual Ear Replicas with Complete Ear Canals Compatible with an Artificial Head," in *Proc. of DAGA 2023*, pp. 166–169, 2023.